Expansion on Reduction of Calcium Doped Lanthanum Chromite

*J. D. Carter, P.V. Hendriksen and M. Mogensen

Materials Department, Risø National Laboratory
P.O. Box 49, DK-4000, Roskilde, Denmark

Danish Energy Agency 1443/92-1

*Present location: Electrochemical Technology Program, Chemical Technology Division
Argonne National Laboratory, 9700 Cass Ave., Argonne IL, 60439
Telephone: (708) 252-6772 Fax: (708) 252-4176

Introduction

Doped lanthanum chromites have been considered as interconnect materials for the solid oxide fuel cell (SOFC) because of their favorable chemical and electrical properties under both oxidizing and reducing environments. Several investigators [1-5] have studied the materials properties of the doped lanthanum chromites to optimize their overall performance as an interconnect material. These properties include electrical conductivity, thermal expansion, sinterability, and chemical compatibility with other cell components. These properties are optimized by the amount of dopants substituted into chromite which are usually Ca or Sr. Figure 1 shows the range of values for these properties.

Another important characteristic becoming more of a concern as investigators are building SOFC stacks is that doped lanthanum chromite expands when reduced in a low oxygen partial pressure (pO_2) ($<10^{-12}$ atm). Plates used to separate oxidizing and fuel gases can deform because of the pO_2 gradient across the interconnect material (Figure 2).

This presentation is a summary of work which will be presented at the Fourth International Symposium on Solid Oxide Fuel Cells [6]. In this article, the possible causes of expansion on reduction of the interconnect will be discussed by using a two-dimensional crystal model. The biaxial strain of the stack is calculated under the assumption that the cell components are forced to remain planar. From this, the maximum stress buildup in the interconnect and electrolyte is estimated. In addition, the effects of thermal expansion mismatch and expansion on reduction of the interconnect are compared, and the optimum interconnect composition from a mechanical standpoint is reported.

Theory of pO_2 Expansion

Defect model The defect chemistry of doped lanthanum chromites can identify the possible chemical species which could cause lattice expansion during the reduction process. This has been characterized by Flandermeyer, Mizusaki, and others [7,8]. In short, the substitution of alkaline earth elements in lanthanum chromite promotes electrical conductivity by the creation of small polaron holes or Cr^{4+} ions to compensate for the reduced charge of the dopant ions. This is illustrated in the left-hand side of equation (1). When the material is reduced in low oxygen

DISCLAIMER

Portions of this document may be illegible in electronic image products. Images are produced from the best available original document.

atmospheres, oxygen is withdrawn from the lattice, and the charges on the newly created oxygen vacancies are compensated by the reduction of two Cr^{4+} ions to Cr^{3+}:

$$La^{3+}_{1-x}Ca^{2+}_{x}Cr^{3+}_{1-x}Cr^{4+}_{x}O_3 \leftrightarrow La^{3+}_{1-x}Ca^{2+}_{x}Cr^{3+}_{1-x+2\delta}Cr^{4+}_{x-2\delta}O_{3-\delta} + \tfrac{\delta}{2}O_2 \quad (1)$$

Using Kröger-Vink notation [9], equation (1) can be rewritten:

$$2Cr^{\bullet}_{Cr} + O^{\times}_{O} \leftrightarrow 2Cr^{\times}_{Cr} + V^{\bullet\bullet}_{O} + \tfrac{1}{2}O_2 \quad (2)$$

The subscripts Cr and O label their respective crystallographic sites, and the superscripts • and × represent a net positive charge and a net null charge, respectively. The V denotes a vacancy, in this case on the oxygen site. Here, formation of oxygen vacancies and the reduction of chromium are possible causes of expansion.

Crystallographic model Glazer [10] has described the structural differences and changes in perovskites by considering (i) the tilting of anion octahedra, (ii) the displacements of B cations (ferroelectric and antiferroelectric behavior), and (iii) octahedral distortions. Figure 3 is constructed according to this model, although (ii) is not relevant here. For simplicity, a two-dimensional representation of the rhombohedral structure of Ca-doped $LaCrO_3$ is drawn. The tilted diamonds represent the oxygen octahedra surrounding Cr ions. The larger open circles represent La^{3+}, and the smaller shaded circle represents Ca^{2+}. The small square represents an oxygen vacancy. It should be noted that the radii, octahedra size, and tilt angles are not drawn to scale.

With reference to Figure 3 and equation (1), as Ca^{2+} is substituted for La^{3+}, a Cr^{3+} is oxidized to Cr^{4+} to compensate for the charge difference. The Ca^{2+} ion has a slightly smaller radius than La^{3+}, as does the Cr^{4+} when compared to Cr^{3+}[11]. These effects may explain why the lattice volume decreases as Ca doping increases [12]. In the case of Sr doping, the Sr^{2+} is larger than the La^{3+}, yet the lattice volume decreases with increasing Sr dopant [13]. This implies that the Cr^{3+} to Cr^{4+} substitution has a greater effect on the lattice size than does La substitution. In addition, Ca and Sr on the La site also have a lower bond strength, as calculated from Pauling's electrostatic valence rule [14]. The reduced bond strengths may account for an increased thermal expansion coefficient with increasing Ca addition [2].

As the chromite is reduced in low pO_2 atmospheres, oxygen vacancies form and two Cr^{4+} ions are reduced to Cr^{3+}. The accompanying expansion has two possible explanations. First, the lattice could expand due to the swelling of the chromium-containing oxygen octahedra as Cr^{4+} is reduced to Cr^{3+}. Here, both the reduced bond strength and the increased ionic radius can contribute to the increased octahedron size. It is believed that the size change of the oxygen octahedra due to the Cr^{4+} to Cr^{3+} transition has a large effect on the lattice size.

Another possibility is that, as oxygen is removed from the lattice, two opposing Cr^{3+} repel each other and rotate their octahedra to increase their linear distance, resulting in a net lattice

expansion. This rotation could change the symmetry of the lattice. In situ crystallographic studies are needed to determine the extent of each effect.

Determination of Overall Expansion

Determination of pO_2 Profile An oxygen permeation model developed by van Hassel et al. [15] was used to calculate the pO_2 through the cross section of the plate in a pO_2 gradient. From equation (2) the equilibrium constant, K, can be written:

$$K = \frac{[Cr_{Cr}^{\bullet}]^2 [V_O^{\bullet\bullet}] (pO_2)^{1/2}}{[Cr_{Cr}^{\bullet}]^2 [O_O^{\times}]} \tag{3}$$

Substituting the subscripts from equation (1) for the concentrations yields the following:

$$K = \frac{(1-x+2\delta)^2 \delta (pO_2)^{1/2}}{(x-2\delta)^2 (3-\delta)} \tag{4}$$

By considering the hole concentration $p = x - 2\delta$:

$$K = \frac{(1-p)^2 (x-p) (pO_2)^{1/2}}{(p)^2 (6-x+p)} \tag{5}$$

Equations (4) and (5) represent two methods of obtaining the equilibrium constant. By using thermogravimetric analysis, one can measure the oxygen weight loss, δ, at a given pO_2 and K can be determined from equation (4) for each composition by least squares fitting. Also, K can be determined in a similar way with equation (5) by using electrical conductivity vs. pO_2 data. The electrical conductivity is given by:

$$\sigma_e = \frac{Fp\mu}{V_m} \tag{6}$$

where F is Faraday's constant, μ is the mobility determined from air measurements and assumed to remain constant, and V_m is the molar volume. From the data of Yasuda [16], the equilibrium constants for $La_{1-x}Ca_xCrO_3$ were determined to be $K = 2 \cdot 10^{-8}$, $6 \cdot 10^{-8}$, and $9 \cdot 10^{-8}$ for x = 0.1, 0.2, and 0.3, respectively.

The flux of oxygen through $La_{1-x}Ca_xCrO_3$ was derived by van Hassel et al. [15] to be:

$$J_{O^{2-}} = -\frac{2FD_v}{LV_m}\left[x \ln\left(\frac{x-2\delta_L}{x-2\delta_0}\right) + 3\ln\left(\frac{3-\delta_L}{3-\delta_0}\right) + (1-x)\ln\left(\frac{1-x+2\delta_L}{1-x+2\delta_0}\right)\right] \tag{7}$$

where D_v is the volume diffusion coefficient, δ_0 and δ_L are the oxygen vacancy concentrations at y = 0 and L, respectively, and y refers to a position in the plate of thickness L. Under steady-state conditions, the oxygen flux is assumed to be constant at any position y within the plate. With this assumption, equations (4) and (7) can be used to determine the variation of defects, δ, and pO_2 as a function of the position y, perpendicular to the planar surfaces of the plate.

Determination of biaxial strain The expansion of the material due to reduction at low pO_2 is mechanically equivalent to thermal expansion in a temperature gradient. Relations derived for thermal strain [17] were used to describe the overall expansion of a SOFC stack on reduction. Assuming that the stack is forced to remain planar and the shear stresses can be neglected, the overall strain will be independent of y or biaxial [6]. The shear stresses can be assumed negligible, except for a few layer thicknesses near the edges of the plate. From force equilibrium, the biaxial strain, ε, of a stack of N layers is obtained:

$$\varepsilon = \frac{\frac{E_N L_N}{1-\nu_N}}{\sum_{j=1}^{N} \frac{E_j L_j}{1-\nu_j}} \int_0^1 \varepsilon^{\delta}(y/L_N)\, d(y/L_N) \qquad (8)$$

where E_j is Young's modulus, ν_j is Poisson's ratio, L_j is the thickness of a given stack component j, and j = N refers to the interconnect plate ($L_N = L$). The function $\varepsilon^{\delta}(y/L_N)$ is the linear expansion of a volume element at position y as a result of the local deviation from stoichiometry. The volume element is assumed to expand independent of the rest of the body. The fraction in front of the integral is referred to hereafter as the "stiffness factor". A stiffness factor of 1 suggests that the overall expansion of the stack is determined exclusively by the expansion of the interconnect and that the restraining action of the other components is negligible. Increasing the restraining effects of the cell would decrease the value of the stiffness factor to a fraction less than 1. The lower limit of the stiffness value is estimated to be about 0.8 for the following: stack geometry, $L_{anode} = L_{cathode} = 50\ \mu m$, $L_{electrolyte} = 150\ \mu m$ (8 mol% yttria stabilized zirconia or YSZ) and $L_N = 3$ mm, elastic constants, $E_{anode}=E_{cathode}= 50$ GPa (small value because of their high porosity), $E_{YSZ} = 200$ GPa (room temperature value [18]), and $E_N = 50$ GPa (estimated high temperature value [19]); and $\nu = 0.3$ for all the SOFC components. The actual stiffness is believed to lie somewhere between these limits.

Results and Discussion

Sintered specimens of $La_{1-x}Ca_xCrO_3$ with x = 0 to 0.3 were heated in a dilatometer and held at a constant temperature of 1000°C. The linear displacement was recorded as the pO_2 varied between $10^{-0.67}$ and 10^{-18} atm. The gas compositions included various mixtures of air, N_2, 3% H_2O and 9% H_2 in N_2. Undoped $LaCrO_3$ showed no expansion effect when reduced in a pO_2 of 10^{-18} atm. However, the expansion due to reduction increased with increasing Ca content (Figure 4). The expansion can be fitted to the equation:

$$\Delta L/L = c\delta \qquad (9)$$

where δ is the deviation from the oxygen stoichiometry, and c is a fitting parameter ranging from 2 (at x = 0.24) to 2.5 (at x = 0.1). Although this equation expresses the dependence on the oxygen nonstoichiometry, it may also show a dependence on the Cr^{3+} concentration. As crystallographic data are obtained, the proper weight of these effects will become apparent.

Equations (8), (9) and the defect profile in the plate were used to calculate the overall expansion of the stack for two different pO_2's (10^{-15} and 10^{-18} atm). The results are plotted in Figure 5 as a function of Ca content. The double symbols represent the upper and lower limits of the stiffness values (1 and 0.8). Comparison of Figures 4 and 5 shows that the overall expansion (ε) is approximately 50-80% of the measured expansion ($\Delta L/L$).

To determine whether or not these magnitudes of expansion are detrimental, it is necessary to compute the resulting stresses in the interconnect and the electrolyte, and compare them to their fracture strengths. If the stack components are kept planar, the chromite interconnect will have a maximum tensile stress on the air side (y=0) of the plate. The YSZ plate will also be under tension. The stresses induced into the stack were estimated by using the aforementioned elastic constants and geometric values according to the equation:

$$\sigma_j(y) = \frac{E_j}{1-\nu_j}[\varepsilon - \varepsilon^{\delta}(y)] \tag{10}$$

In this equation, $\varepsilon^{\delta}(y) = 0$ when referring to stack components other than the interconnect ($j \neq N$). Table I shows the estimates of the maximum tensile stress values in $La_{1-x}Ca_xCrO_3$ and YSZ. Dokiya reported that the strengths of tape-cast $La_{1-x}Ca_xCrO_3$ foils are 30 to 130 MPa in air and 20 to 50 MPa in H_2 at 1000°C [20]. The electrolyte has a room-temperature strength on the order of 240 MPa [21]. From these estimates, it can be seen that the stresses imposed due to expansion on reduction can exceed the strengths of these materials. In other words, crack formation in the interconnect or the electrolyte plates is likely to occur for high Ca doping.

To minimize the effects of expansion on reduction the Ca content should be minimized. However, since thermal expansion matching between the YSZ electrolyte and $La_{1-x}Ca_xCrO_3$ is also a mechanical issue, there must be a compromise with the chromite composition. The elastic strain in the YSZ introduced by the mismatch between the thermal expansion coefficients of YSZ and $La_{1-x}Ca_xCrO_3$ is approximately [6]:

$$\varepsilon = (\alpha_{LC} - \alpha_{YSZ})\Delta T \tag{11}$$

where a stiffness factor of 1 is assumed; α_{LC} and α_{YSZ} are the thermal expansion coefficients of $La_{1-x}Ca_xCrO_3$ and YSZ, respectively; and ΔT is the temperature change between the stack bonding temperature and room temperature (25-1000°C). Using $\alpha_{YSZ} = 10.8 \times 10^{-6}/°C$ [22] and thermal expansion data on $(La_{1-x}Ca_x)CrO_3$ [2], we determined the strain in the YSZ due to thermal expansion mismatch as a function of Ca content (dashed line in figure 5).

As indicated by the dashed line in Figure 5, the optimum composition of $La_{1-x}Ca_xCrO_3$ for obtaining minimal strain occurs at x = 0.20 to 0.25.

Conclusions

Defect chemistry and a crystallographic model were used to identify the possible causes of expansion on reduction of doped $LaCrO_3$ materials. Measurements of expansion during reduction of $La_{1-x}Ca_xCrO_3$ showed values ranging from 0 to 0.30% for x = 0 to 0.30, respectively. When a chromite plate is subjected to a pO_2 gradient ($1\text{-}10^{-15}$ atm) and is constrained to remain planar, as in the case of a SOFC stack, only 50-80% of the above expansion is realized. The stresses building up in both the interconnect and electrolyte lie within the range of the reported strengths, and therefore, cracking is expected to be observed in either of the components for high Ca doping levels. Doping levels of x = 0.20 to 0.25 were determined as a compromise between the expansion on reduction effects and the mismatch of the thermal expansion.

Acknowledgment

Special thanks to J.D. Jorgensen for helpful discussions on the crystallographic model.

References

[1] W. Schafer and R. Schmidberger, "Ca and Sr Doped $LaCrO_3$: Preparation, Properties and High Temperature Applications," *High Tech Ceramics*, edited by P. Vincenzini, pp. 1737-42 (Amsterdam, Elsevier Science Publishers, 1987).

[2] N. Sakai, T. Kawada, H. Yokokawa, M. Dokiya, and T. Iwata, "Thermal Expansion of Some Chromium Deficient Lanthanum Chromites," *Solid State Ionics* **40/41** 394-397 (1990).

[3] N. Sakai, T. Kawada, H. Yokokawa, M. Dokiya, and I. Kojima, "Liquid-Phase-Assisted Sintering of Calcium-Doped Lanthanum Chromites," *J. Am. Ceram. Soc.* **76** [3], 609-616 (1993).

[4] J.D. Carter, "A Low Temperature Sintering Aid for Calcium Doped Lanthanum Chromite," D.K. Patent 930943 A (August 18, 1993).

[5] J.D. Carter, C. Clausen, and M. Mogensen, "Calcium Reactions at the Calcium Doped Lanthanum Chromite-Yttria Stabilized Zirconia Interface," *Proceedings of the 14th Risø International Symposium on Material Science: High Temperature Electrochemical Behaviour of Fast Ion and Mixed Conductors*, edited by F. W. Poulsen, et al., pp. 223-228 (Risø National Laboratory, Denmark, 1993).

[6] P.V. Hendriksen, J.D. Carter, and M. Mogensen, "Dimensional Instability of Doped Lanthanum Chromites in an Oxygen Pressure Gradient," to be presented at the Fourth International Symposium on Solid Oxide Fuel Cells, Yokohama, Japan, June 18-23, 1995.

[7] B.K. Flandermeyer, M.M. Nasrallah, A.K. Agarwal, and H.U. Anderson, "Defect Structure of Mg-Doped $LaCrO_3$: Model and Thermogravimetric Measurements," *J. Am. Ceram. Soc.* **67**, 195-198 (1984).

[8] J. Mizusaki, S. Yamauchi, K. Fueki and A. Ishikawa, "Nonstoichiometry of the Perovskite-type Oxide $La_{1-x}Sr_xCrO_{3-\delta}$," *Solid State Ionics* **12**, 119-124 (1984).

[9] F.A. Kröger, and H.J. Vink in *Solid State Physics Vol 3*, edited by F. Seitz and D. Turnbull, p. 307 (Academic Press, New York, 1965).

[10] A.M. Glazer, "Simple Ways of Determining Perovskite Structures," *Acta Cryst.* **A31**, 756-762 (1975).

[11] R.D. Shannon, "Revised Effective Ionic Radii and Systematic Studies of Interatomic Distances in Halides and Chalcogenides," *Acta Cryst.* **A32**, 751-767 (1976).

[12] J.D. Carter, V. Sprenkle, M. M. Nasrallah, and H. U. Anderson, "Solubility of Calcium in Lanthanum Chromite," *Proceedings of the Third International Symposium on Solid Oxide Fuel Cells*, Vol 93-4, Edited by S.C. Singhal, and H. Iwahara, pp 344-353, (Pennington, NJ: The Electrochemical Society, 1993).

[13] C. Khattak and D. Cox, "Structural Studies of the (La,Sr)CrO_3 System," *Mat. Res. Bull.* **12**, 463-472 (1977).

[14] Cited in A.R. West, *Basic Solid State Chemistry*, p. 95 (John Wiley, New York, 1988).

[15] B.A. van Hassel, T. Kawada, N. Sakai, H. Yokokawa and M. Dokiya, "Oxygen Permeation Modelling of $La_{1-y}Ca_yCrO_{3-\delta}$," *Solid State Ionics* **66**, 41-47 (1993).

[16] I. Yasuda, and T. Hikita, "Electrical Conductivity and Oxygen Chemical Diffusion Coefficient of Calcium-Doped Lanthanum Chromites," *Proceedings of the Second International Symposium on Solid Oxide Fuel Cells*, edited by F. Gross et al., pp. 645-652 (Commission of the European Communities, Luxembourg, 1991).

[17] S.S. Manson, *Thermal Stress and Low-cycle Fatigue* (McGraw Hill, New York, 1966).

[18] E. Scafe, M. Brocco, G. Cosoli and, M. Ronchetti, Proceedings of the 6th IEA Workshop on Solid Oxide Fuel Cells, Rome, p. 307 (1994).

[19] C.S. Monstross, H. Yokokawa, and M. Dokiya, 2nd Symposium on Solid Oxide Fuels Cells in Japan, extended abstract 214A (1993).

[20] M. Dokiya, T. Horita, N. Sakai, T. Kawada, H. Yokokawa, B.A. van Hassel, and C.S. Montross, "Interconnector Chemistry", *Proceedings of the 14th Risø International Symposium on Material Science: High Temperature Electrochemical Behaviour of Fast Ion and Mixed Conductors*, edited by F. W. Poulsen et al., pp. 33-41 (Risø National Laboratory, Denmark, 1993).

[21] D. Stolten, E. Monreal and W. Muller, Programs and Abstracts, 1992 Fuel Cell Seminar, Tucson, AZ, edited by C.E. Pax (Courtesy Asso. Inc., Washington D.C., 1992).

[22] M. Mogensen, T. Lindegaard, U.R. Hansen and G. Mogensen, *J. Electrochem. Soc.* **141** 2122 (1994).

Important properties of $La_{1-x}Ca_xCrO_3$ inteconnects
- These depend on dopant concentration -

- Electrical conductivity: σ_e ~ **1 to 60 S/cm at 1000°C**

  in oxygen pressures of: **pO_2 ~ 10^{-18} to 1 atm O_2**
- Thermal expansion : **α ~ 9 to 10.8·10^{-6}/°C**
- Sinter density: $\rho_s \geq$ **95% at 1450°C**
- Compatible when single phase

Figure 1.

The effects of expansion on reduction of a $La_{1-x}Ca_xCrO_3$ interconnect plate

Figure 2.

$La_{1-x}Ca_xCrO_3$ crystal structure model

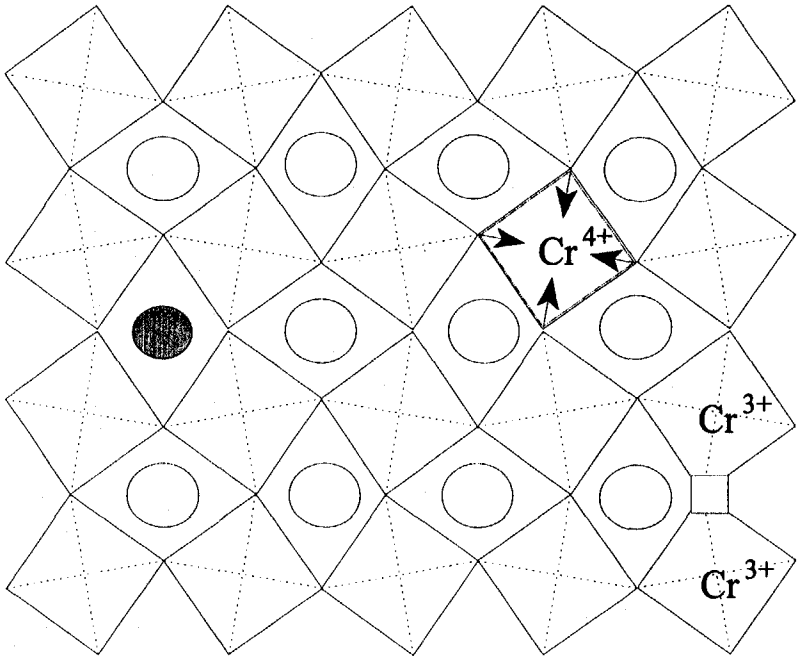

		Ionic radius (Å)	Bond Strength
La^{3+}=	○	1.36	3/12
Ca^{2+}=	●	1.34	2/12
Cr^{3+}		0.62	3/6
Cr^{4+}		0.55	4/6

Figure 3.

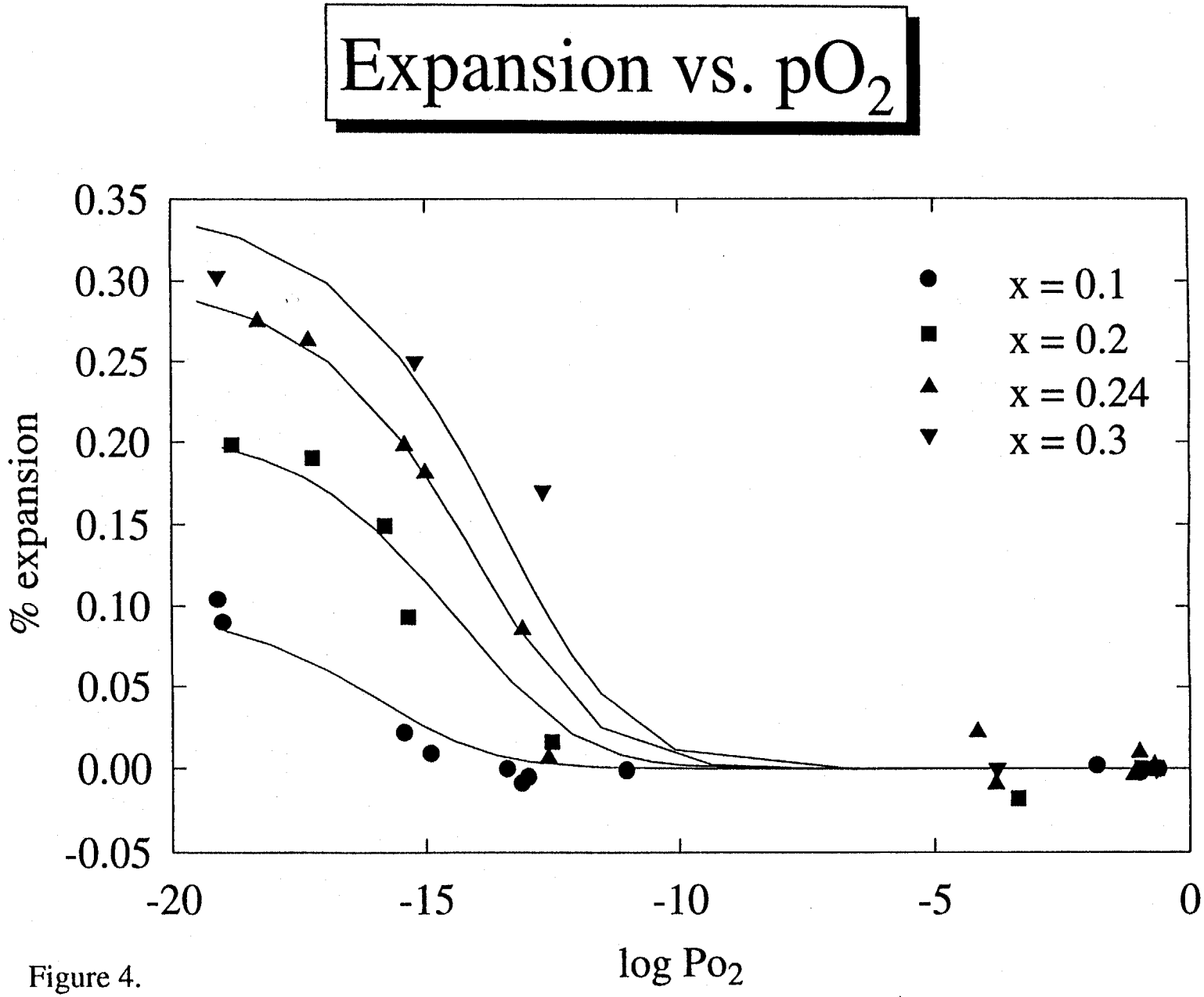
Expansion vs. pO2
0.35
0.30
0.25
0.20
0.15
0.10
0.05
0.00
-0.05
% expansion
-20
-15
-10
-5
0
log Po2
x = 0.1
x = 0.2
x = 0.24
x = 0.3

Figure 4.

Overall Expansion vs. Ca Content

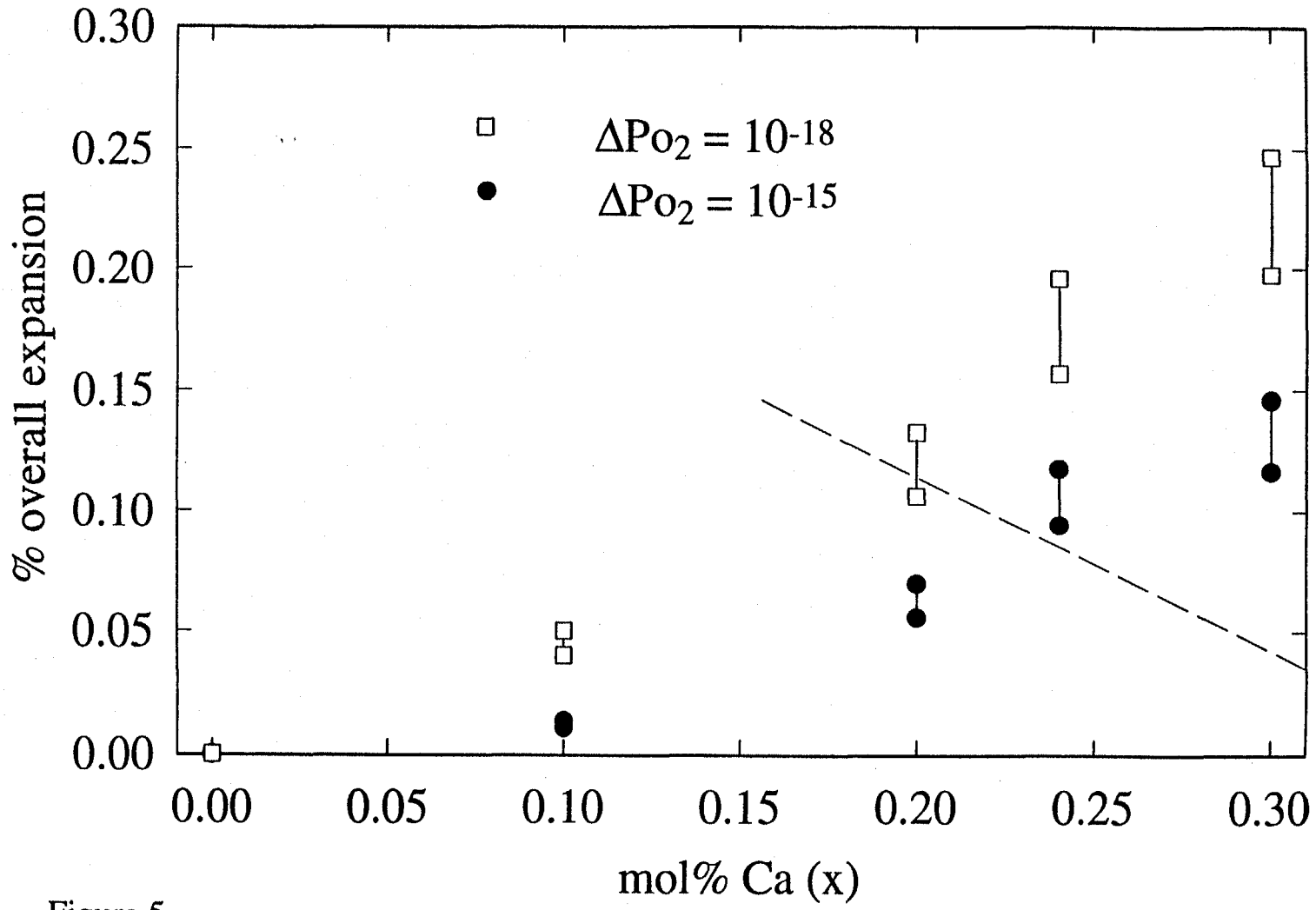

Figure 5.

Estimated maxium tensile stresses in
$La_{1-x}Ca_xCrO_3$ and YSZ plates
fuel cell conditions: $\Delta pO_2 = 10^{-15}$ atm, 1000°C

Chromite Composition (x)	Maximum Tensile Stress (MPa)	
	$La_{1-x}Ca_xCrO_3$	YSZ
0.1	10	20
0.2	50	140
0.24	80	240
0.30	100	300
Maximum Strengths	(30-130)[20]	(240)[21] (room temp)

Table I.